Self-standing gelatin- methacryloyl 3D structure using Carbopol-embedded printing

Self-standing methacrylated gelatin (GelMA) 3D structure using Carbopol-embedded printing

Simona Villata[1], Francesca Frascella *[1] Cesare Gabriele Gaglio[1], Giuliana Nastasi[1], Mauro Petretta[3], Candido Fabrizio Pirri[1,2], Désirée Baruffaldi[1]

*Corresponding author: francesca.frascella@polito.it

[1] DISAT - PolitoBIOMed Lab – Politecnico di Torino, Corso Duca degli Abruzzi 24, 10129 Turin, Italy

[2] Center for Sustainable Future Technologies, Italian Institute of Technology, Via Livorno 60, 10144 Turin, Italy

[3] REGENHU SA, Z.I Du Vivier 22, CH-1690 Villaz-St-Pierre, Switzerland

Abstract

Methacrylated gelatin (GelMA) hydrogel has gained huge success in the last decades thanks to its versatilities in many applications. Notably, one of them is 3D bioprinting, as GelMA physical-mechanical properties and biocompatibility of uncured formulation perfectly suit the requirements of a bioink. Nevertheless, before the photopolymerization, the hydrogel shows weak mechanical properties and long recovery–time after stress application, which results in the inability to obtain complex and self-standing forms due to structure collapse. In this work, Carbopol ETD 2020 NF, dissolved in cell culture medium, was used as supporting bath to optimize GelMA bioprinting and overcome its stability limitations. The achieved results demonstrated the possibility of printing shapes containing hollows with lumens or non-planar surfaces, also by using nozzles with larger inner diameter, which reduced cell death during printing process, but were usually avoid because of low resolution. Moreover, constructs' extraction was easier when Carbopol solution was prepared in culture medium rather than in water, reducing sample handling. In conclusion, thanks to this supporting bath, it was possible to print cellularized scaffold, with channels that were then seeded, obtaining inner structure. Further, this Carbopol formulation could be considered an eligible candidate as a supporting bath to obtain GelMA 3D self-standing-shaped and vascularized scaffold.

Graphical abstract

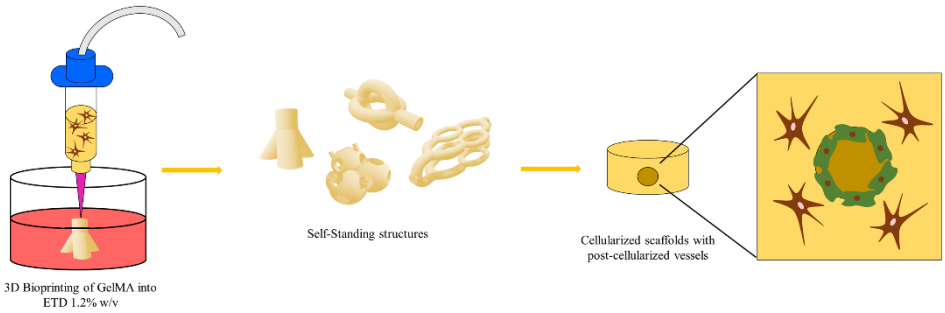

Keywords: **3D bioprinting, supporting bath, GelMA, Carbopol**

1. Introduction

Nowadays, 3D *in vitro* models and engineered tissue are gaining huge relevance in the field of bioengineering, since cells growing on 2D flat substrates are far from mimicking the *in vivo* status [1]. Moreover, with the development of 3D culture systems, the possibility to spatially pattern cells and their matrix quickly becomes one of the main requirements in the field [2]. To face it, 3D bioprinting took a very special place in the scenario of the life sciences, with the aim of being able to print whole tissues and organs [3]. Many techniques for 3D bioprinting have been explored [4], but the most widely used for tissue engineering applications, is extrusion-based bioprinting [5]. The main component of this technique is the bioink, defined as a formulation of cells and an

acellular biomaterial component [6]. To perform bioprinting, the bioink is loaded into a cartridge equipped with a needle and extruded in a layered pattern to build the 3D construct [7]. Usually, the materials employed are hydrogels since they can entrap large amounts of water, a key property to provide biomimetic environments for living and functional cells [2].

Many materials eligible as bioinks have been developed and synthesized [8], trying to reach the optimal trade-off between cellular survival and growth, printability and mechanical stability. Notably, methacrylated gelatin (GelMA) has achieved a tremendous success for this purpose, becoming one of the most broadly used materials for 3D bioprinting [3,9–12]. Its main advantages are the great cytocompatibility, the easy and tunable synthesis and the possibility of crosslinking through photopolymerization, which is essential to achieve mechanical stability during long-term cell culture [13,14]. Back to the trade-off between cell viability and mechanical properties, it is known that the biological function is achieved if the acellularized component properties match the extracellular matrix features [15]. This leads to a not so wide collection of materials. Moreover, printing parameters, such as temperature and pressure, must fit within a limited range to not harm the cellular part [15]. Special focus must be put on the nozzle used to perform bioprinting. Evidence shows that the cells experience higher shear stresses for a greater portion of the nozzle length in the straight needles compared to the tapered ones and, moreover, increasing the nozzle diameter, shear stress decreases, leading to a lower impact on cell viability. However, a larger nozzle diameter negatively affects printing resolution [16].

Basically, improving resolution and mechanical stability of the bioprinted structures is necessary to obtain more complex shapes with high fidelity [17]. Some attempts have employed materials as sacrificial inks both to improve structure fidelity and to create more complex structures such as vascular networks or inner linings [18,19].The side effects of these approaches are that they often introduce a further level of complexity, for instance, the need of more than one printhead, and technical difficulties during printing and in the post-print treatments [20].

A novel and groundbreaking technique is represented by embedded printing [17,20–22], in which bioprinting is performed in a supporting bath that provides physical confinement of the ink. This has been shown to increase print resolution and fidelity [17,23], but also to prevent structural collapsing, enabling the fabrication of more complex structures, lowering the interfacial tension between the ink and the surrounding environment, usually air [17]. The supporting bath generally is a yield stress fluid: when the movement of the nozzle generates a shear stress that exceeds the yield stress of the supporting bath, the latter temporarily changes in proximity of the nozzle from a solid-like state to a fluid-like one. Due to this, the bioink can be deposited in the supporting bath, and, since the material returns to its solid-like state when the nozzle moves to another, the printed inks are trapped, forming a 3D structure that can resist gravitational deformation [21]. Selecting the ideal material for the supporting bath poses a significant challenge due to several requirements, especially concerning the rheological properties [17]. One of the primary requirements is that the elastic shear modulus, or storage modulus (G'), of the supporting bath material has to be sufficiently high to support the bioink. Also, if the bath's G' is too lower than the bioink's one, the extruded ink could drag through the support bath, resulting in the loss of resolution and limitation in complex shape formation. Conversely, if the bath's G' is higher than that of the bioink, the needle will form a crevice, and the liquid-like ink may flow upward, leading to the loss of upper confinement [24,25]. The rheological properties more linked with the nozzle movement are the yield stress and the recovery time [17]. The first one represents the shear stress needs for flow initiation: if a stress is not applied or it is below the yield stress, the bath material will show solid-like properties, conversely, when the applied stress is above the yield stress, the bath material will begin to flow. It needs to be taken into consideration that, to perform embedded bioprinting, the bath material must have a yield stress, even if it is low [26]. As said before, when the nozzle changes its position is crucial that the bath returns to its solid-like properties to confine the extruded ink. For this reason, the last important rheological property is the recovery time, defined as the time it takes for the viscosity or modulus of the material to return to its original value after that a high shear rate has been applied [17]. This amount of time should be minimized as this ensures that the extruded ink remains confined after printing [27].

Carbopol is a soft granular microgel, made from high molecular weight, poly (acrylic acid) polymers [28]. It is hydrophilic, so it reaches maximum swelling in aqueous solution around neutral pH, therefore it can be dissolved in water [20,29–32] or cellular medium [23,28]. Carbopol has already been used as support bath in embedded bioprinting application [16,20,23,30–32]. However, many investigations [20,29–32] dissolve Carbopol in distilled water, that could lead to some problems, like osmotic stress to the cellular component [33]. However, Carbopol dissolved in cell culture medium has weakly been explored, and only as a bioink [28] or a so-called liquid-like solid growth medium to print directly cells that, in this way, are not tightly confined inside a bioink [34]. In this study Carbopol prepared in cell culture medium has been used as a support bath for cell laden GelMA bioprinting, to avoid the drawbacks of water (i.e. osmotic stress on cells) and at the same time, to preserve printing fidelity

even with a nozzle with larger diameter and to allow the maintenance of self-standing structure before the photopolymerization.

2. Material and methods

2.1 GelMA synthesis

GelMa was synthesized as previously reported [13]. Briefly, 10 g of type B gelatin from bovine skin (Sigma Aldrich, gel strength 50–120 bloom) was dissolved into 100 ml of Dulbecco's Phosphate Buffered Saline (DPBS, Sigma Aldrich) to obtain a concentration of 10% w/v at 50°C for 1h. To introduce methacryloyl groups to gelatin's reactive amine and hydroxyl groups, 8 ml of Methacrylic Anhydride (MA, Sigma Aldrich) was added to the previous solution drop wisely under continuous stirring to obtain a degree of functionalization of 90.6 +/- 0.77. The reaction lasted 2 hours in the dark at 40°C, then was stopped by diluting the reaction mixture with an equal volume of DPBS (i.e., 100 mL). The resulting solution was dialyzed against ddH_2O with cellulose membrane (12–14 kDa molecular weight cutoff, Sigma Aldrich) for 1 week at 40°C, to completely remove unreacted MA. Finally, GelMA was freeze-dried and kept at room temperature (RT) until use.

2.2 Carbopol (EDT 2020 NF) preparation

Carbopol ETD 2020 NF, kindly provided from Lubrizol Corporation (Wickliffe, OH, USA) was used to prepare the printing bath for the 3D bioprinting, following the previously reported preparation protocol [28]. Briefly, ETD 2020 NF powder, sterilized by UV irradiation, was dissolved in cell culture medium (Gibco BenchStable™ DMEM GlutaMAX™ medium) or sterile double distilled water (ddH_2O) at the concentration of 1.2% w/v or 0.4 % w/v, respectively. The ETD 2020 NF concentration in ddH_2O used has been previously optimized by Brunel and colleagues[17]. Due to its anionic nature, the polyelectrolyte polymer solution obtained resulted in a highly acid solution. For this reason, it had to be neutralized with NaOH 5 M to obtain a physiological pH, at which it showed the maximum swelling and high viscosity.

2.3 Rheological characterization

Rheological measurements were performed using an Anton Paar rheometer (Physica MCR 302) at a constant temperature of 12°C and in parallel-plate mode with a 0.3 mm gap between two aluminum plates (both with a diameter of 20 mm). To measure the storage modulus (G'), oscillatory tests were performed at a constant frequency of 1 Hz, ranging from a strain of 0.01–1000 %. For the yield stress measurement, rotational tests were performed at a constant frequency of 1 Hz ranging from a shear stress of 1 Pa until 10000 Pa. Shear thinning behavior was tested by setting the shear rate range from 1 to 1000 s^{-1}. In the end, a thixotropic curve was obtained by applying a shear rate of 1 s^{-1} for 25 s, of 100 s^{-1} for 50 s, and again 1 s^{-1} until the end of the measurement. All experiments were performed at least three times.

2.4 Absorbance

100 µl of ETD 2020 NF dissolved in ddH_2O or DMEM at the concentration of 0.4% w/v and 1.2% w/v, respectively and already neutralized with NaOH 5 M, were transferred in a 96-well plate (TC treated, Greiner Bio-One) and the absorbance spectra of the materials were measured from 300 nm to 500 nm using Synergy™ HTX Fluorescence Multi-Mode Microplate Reader. 100 µl of solution of lithium phenyl-2,4,6-trimethylbenzoylphosphinate (LAP) dissolved in DMEM at the concentration of 2,5 mg/ml was used as positive control.

2.5 Cell culture

Human lung adenocarcinoma cell lines, A549-GFP^+ were kindly provided by Dr. Valentina Monica, Department of Oncology, University of Torino, AOU San Luigi Gonzaga. For A549-GFP^+, A549 were infected to constitutively express histonic protein H2B fused with the green fluorescent protein (GFP). Both cell lines were cultured in Gibco BenchStable™ RPMI 1640 GlutaMAX™ medium (Thermo Fisher) supplemented with 10% Fetal Bovine Serum and 1% penicillin/streptomycin (all from Sigma Aldrich).
Human dermal fibroblasts HFF-1 (ATCC) were cultured in Gibco BenchStable™ DMEM GlutaMAX™ medium (Thermo Fisher) supplemented with 15% Fetal Bovine Serum, 1% L-Glutamine, 1% Sodium Pyruvate and 1% penicillin/streptomycin (all from Sigma Aldrich).

All cell lines were cultured in a humidified incubator at 37°C, 5% CO_2 and they were periodically checked for mycoplasma contamination.

2.6 GelMA bioink preparation

GelMA hydrogel was obtained as previously shown [35]. Specifically, freeze-dried GelMA was dissolved at the concentration of 10% w/v in Gibco BenchStable™ DMEM GlutaMAX™ medium (Thermo Fisher), previously supplemented with lithium phenyl-2,4,6-trimethylbenzoylphosphinate (LAP, Sigma Aldrich) as photoinitiator at the concentration of 2.5 mg/mL. The solution was heated at 60°C for 30 minutes and filtered through 0.45 µm and 0.22 µm PES membrane filters (Asimo) to sterilize it. All GelMA solutions were pre-warmed at 37°C before cells embedding.

2.7 Viability analysis

The biocompatibility of ETD 2020 NF solutions in ddH_2O and DMEM was assessed as previously described [28]. Briefly, HFF-1 or A549 GFP^+ were suspended in the formulations at the density of $3x10^6$ cells/ml. MTT at the concentration of 0,5 mg/ml in DMEM was used to evaluate the viability at each time point. After 3 h of incubation at 37°C, the formazan salts were dissolved in 200 µl of DMSO and the absorbance at 570 nm (650 nm reference wavelength) using Synergy™ HTX Fluorescence Multi-Mode Microplate Reader.
The viability of cells embedded in printed GelMA, prepared in DMEM at the concentration of 10 % w/v, was evaluated by Live/Dead staining kit (Sigma-Aldrich) after 1 and 14 days of culture. Specifically, reagents were dissolved according to the manufacturer's instruction. The samples were washed twice in DPBS for 5 minutes, then, the staining solution was added and incubated at 37°C for 40 minutes. After a further washing step, the constructs were analyzed by a microscope (Eclipse Ti2 Nikon, Tokyo, Japan) equipped with a Crest X-Light spinning disk confocal microscope and a Lumencor SPECTRA X light engine.

2.8 3D bioprinting and constructs extraction

Different architectures were produced with a 3D discovery bioprinter (RegenHu, Switzerland). CAD models were previously designed with Solidworks SP05.1 to generate STL files and then converted to G-code with the BioCAM software (RegenHu, Switzerland). For the slicing, a rectilinear infill pattern with a 0/90° alternate deposition and a density of 40% was selected. The layer height was set to 0.3 mm, for the non-cellularized self-standing structures, GelMA was extruded using a 3 ml UV-secure pneumatic-driven extrusion printhead and a nozzle with an inner diameter of 250 µm, directly into 6 well suspension plates (Greiner bio-one), filled with ETD 2020 NF formulation. For the cell-laden scaffolds, GelMA was pre-mixed with 1.5×10^6 cell/ml HFF-1 and then extruded using the same printhead and nozzle, directly into 12 well suspension plates (Greiner bio-one) filled with ETD 2020 NF formulation. In both cases, feed rate was 8 mm/s and the printing pressure was approximately 0.080 MPa. GelMA was then photopolymerized for 1 min in a UV oven (Asiga) at λ = 365 nm, 10 mW/cm^2. To extract the samples, sterile DPBS was added on top of ETD 2020 NF to dilute it and then it was aspirated. Other two washes in sterile DPBS were necessary to obtain clean samples. The cell-loaded constructs were then submerged in 2 ml of fresh culture medium and placed in an incubator at 37°C and 5% CO_2. Cell culture medium was replaced every 2 days until the end of the experiments. **Experimentally was assessed that 12°C was the best temperature to obtain the extrusion of a printing-suitable filament.**

2.7 Channels cell seeding

After printing the construct, the channel was washed twice with DPBS and then, A549 GFP^+ cells were resuspended in complete medium at the density of 1×10^5 cells/ 10 µL of complete medium. Then, 10 µL of the prepared mix were added inside the empty channel and the well was filled with 1.5 mL of complete medium. After 24 hours the construct was cut, and the channel analyzed by optic and confocal microscopy.

2.8 SEM

Morphological characterization of GelMA was carried out by field emission scanning electron microscopy (FESEM, Zeiss Supra 40, Oberkochen, Germany). To prepare the samples, they were incubated overnight in cell culture medium to reach maximum swelling, freezed at -80°C and lyophilized. Before the characterization, the samples were coated with a film of Pt/Pd 5 nm thick.

3. Results and discussion

3.1 Rheological characterization

3D bioprinting is an outstanding technique that allows the precise and controlled deposition of cell-loaded biomaterials. Unfortunately, many photocurable bioinks were characterized by low viscosity and poor maintenance of printed structures before the polymerization, which, in turns, results in their exclusion as eligible matrix, despite their biocompatibily. In this scenario, supporting baths represent a promising solution and the choice of the most suitable ones relies on their rheological properties and biocompatibility [17,20–22]. GelMA derived from type B gelatin at the concentration of 10% w/v in cell culture medium (i.e., DMEM) was chosen as matrix for the printing of cell-loaded scaffolds. To assess its printability, the recovery time was verified by rheological analysis, indeed, prolonged time can lead to filament flattening during the printing process before photopolymerization [36]. After being subjected to high shear stresses, GelMA formulation showed a recovery time of 20 s before reaching a plateau of 80% of its original viscosity (230 Pa*s), as shown in Fig 1S., hence, the use of a supporting bath with a sufficiently fast recovery can improve greatly the printing resolution and the maintenance of self-standing structure before the polymerization.

For that reason, the viscoelastic properties of ETD 2020 NF formulation in ddH_2O or in DMEM were characterized. Importantly, the bath must show shear thinning behavior to ensure a decrease in viscosity during printing and to allow the bioink deposition [26,37]. As expected from previous analysis [28,34], ETD 2020 NF exhibits distinct thixotropic behavior, ranging from 47.3 Pa*s and 52.10 Pa*s at a shear rate of 1 s^{-1} for ETD 2020 NF prepared in DMEM and ddH_2O respectively, to 0.26 Pa*s (in both cases) at a shear rate of 1000 s^{-1} (Fig 1a).

Then, an amplitude sweep test was performed to identify the Linear Viscoelastic Region (LVE) and derive the storage moduli (G_{bath}') which must be near to the one of the bioink [17]. Both formulations showed similar G', obtained by calculating the mean in the Linear Viscoelastic Region (LVE). The obtained values were 303.44 Pa +/- 2.1 Pa and 327.13 +/- 2.57 Pa for ETD 2020 NF prepared in DMEM and ddH2O, respectively. Both formulations were compared with GelMA at 10% w/v, which had a mean G_{ink}' of 143.90 +/- 6,29 Pa (Fig 1b). The storage modulus of the support bath, G_{bath}', is higher than the storage modulus of the bioink, G_{ink}', but the difference is compatible with Carbopol use as printing bath.

ETD 2020 NF also displays a distinct yield stress behavior, essential for a supporting bath material that should exhibit a fluid-like state solely during the nozzle's passage through it. Once the ink is deposited by the nozzle, to sustain and prevent gravitational deformation, the supporting bath should promptly revert to a solid-like state [21]. By selecting a shear rate of 1 s^{-1} as threshold for flow initiation, the resulting yield stress was found to be 43.9 Pa and 47.4 Pa for ETD 2020 NF prepared in DMEM and ddH_2O, respectively (Fig 1c).

Regarding the recovery time, a slight difference in formulations behavior was observed. Interestingly, ETD 2020 NF prepared in DMEM showed an immediate recovery of 94.5% of its initial viscosity, while when prepared in ddH_2O, the immediate recovery was observed to be of 81.25%, reaching 93.5% of its initial viscosity after 15 seconds (Fig 1d). Importantly, the bath prepared in ddH_2O may hinder printing at high rates as full recovery time is 15 seconds, possibly leading to insufficient support to the printed structures.

Immediate recovery is also necessary to maintain a good printing fidelity when using tapered needles, which drag higher quantities of material than traditional straight needles but can preserve better cell viability by subjecting them to lower shear stresses. Overall, using ETD 2020 NF prepared in DMEM can provide an advantage by allowing the use of a more suitable needle for bioprinting and by avoiding osmotic stress to which cells may be subjected when ddH_2O is used as a solvent [33].

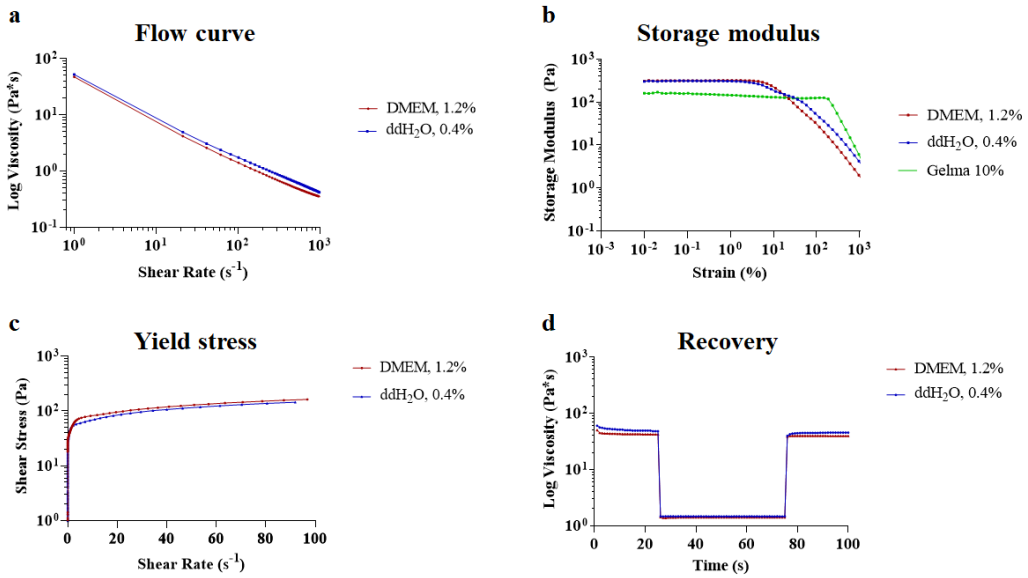

Fig 1 Rheological analysis. (a) Comparison of shear thinning behavior of ETD 2020 NF dissolved in ddH_2O or in DMEM. (b) Evaluation of the storage moduli of the supporting baths and the bioink (GelMA 10% w/v). (c) Assessment of the Yield stress and of (d) the thixotropic behavior to evaluate the recovery of initial viscosity after the application of a stress.

3.2 Supporting bath compatibility with light-induced photopolymerization

As described in Material and Methods section, GelMA crosslinking is induced by the activation of the added photoinitiator, named LAP, when irradiated at 365 nm. For that reason, supporting bath must not interfere with the light irradiation and hydrogel crosslinking. As described in Fig 2 absorbance at 365 nm of both ETD 2020 NF formulations is lower than LAP solution. Thus, they did not interfere with the irradiation, and consequently, with GelMA polymerization.

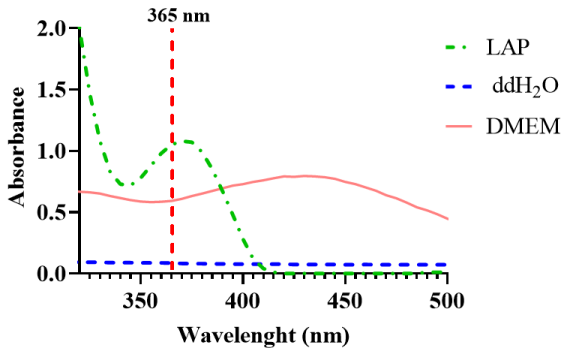

Fig 2 Evaluation of the spectra of the solution of photoinitiator (LAP) dissolved in DMEM at the concentration of 2.5 mg/mL and of the two ETD 2020 NF formulations in ddH_2O or DMEM at the concentration of 0.5 % w/v and 1.2 % w/v respectively.

Although cells were embedded into GelMA hydrogel, the cytocompatibility of the printing bath is mandatory to avoid cell death or toxic effects. Several works already demonstrated the cytocompatibility of ETD 2020 NF formulations in cell culture medium [28,32,34], but the comparison between the two formulation was carried on detecting any advantages related to Carbopol dissolution in ddH_2O or DMEM. As expected, cells embedded into DMEM-based formulation maintained higher viability compared to the one cultured in Carbopol prepared in

ddH_2O (Fig 2S). Since ETD 2020 NF residues could remain after washing steps with DPBS, higher cytocompatibility was preferable for the establishment of functional cell culture models.

3.3 GelMA 3D printing

Since it is well-known that constructs extraction from Carbopol dissolved in water is not easy [22], here GelMA square grids (10 mm of length and 3 mm of thickness) with increasing infill spacing from 1 mm to 3.5 mm were extracted from ETD 2020 NF both dissolved in water (Fig 3 g-n) and in DMEM (Fig 3 o-t), as control, the same grids were printed without the supporting bath (Fig 3 a-f). Importantly, the goal was the printing of grid with nozzles with larger diameter which are more cell-friendly but negatively affect printing resolution [38]. As expected, grid printed with a 250 µm diameter nozzle without the supporting bath did not maintain the desired design (Fig 3 a-f), confirming the need of a different approach. Hence, the outcomes of printing in Carbopol supporting bath were assessed. After the printing step, grids were photopolymerized and extracted. Both supporting baths (Fig 3 g-t) helped to obtain more defined grids. Moreover, constructs extraction showed slight differences: grids were quite difficult to extract when printed in ddH_2O based formulation, further this limitation was exacerbated when the interlinear space was higher, as the bath could not be removed between the printed filament without destroying the construct. On the other side, grids printed into ETD 2020 NF dissolved in DMEM exhibited a better behavior, and it was possible to wash them completely.
Taken together all the results, ETD 2020 NF dissolved in DMEM was selected as supporting bath of election because of its faster recovery after stress application, higher biocompatibility, and easier removal after photopolymerization.

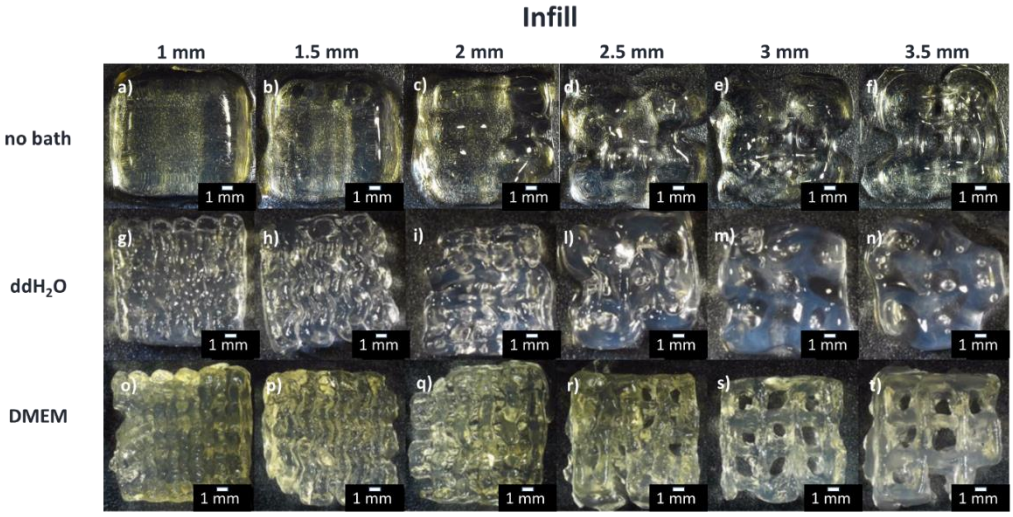

Fig 3 Pictures of GelMA grid printed without the supporting bath (a-f), in ETD 2020 NF ddH_2O (g-n) or in ETD 2020 NF DMEM (o-t) and extracted by Carbopol dilution with cell culture media.

3.4 3D printing of self-standing structure

GelMA has been widely used as bioink in bioengineering, but as mentioned earlier, its major weakness is its mechanical instability before the photocrosslinking, which does not allow to obtain self-standing and complex structures, such as vascular nets or other types of channels and lumens. To overcome this, ETD 2020 NF-DMEM bath was used to print scaffolds with different structure to test different shape fidelity and complexity. As shown in Fig 4, the supporting bath was able to sustain the printing of bigger structure, avoiding the collapse before the photopolymerization, also when the scaffold includes not connected layers at different height (Fig 4 d,h,l).
Afterwards, to further test ETD 2020 NF bath performance, vessels like geometry were fabricated. Cylindrical scaffolds of 1 cm in diameter and 3 mm in thickness were designed, with a rounded channel of 1 mm in diameter at a height of 1.5 mm (i.e., in the middle of the scaffold). Described construct was then printed in the supporting bath, photopolymerized, extracted and, after one day of incubation in cell culture medium to swell, they were cut in half, freeze-dried, and analyzed with SEM, to check the channel morphology [39]. It was observed that the channels were well-formed and through-hole, with height only 0.5 mm and length 1.5 mm (Fig 5). This difference

could be associated with a slight collapsing of the channel due to the upper GelMA weight. However, this approach succeeded in sustaining GelMA during channel fabrication without the need for additional sacrificial inks, making this technique eligible for the printing of vascularized scaffolds.

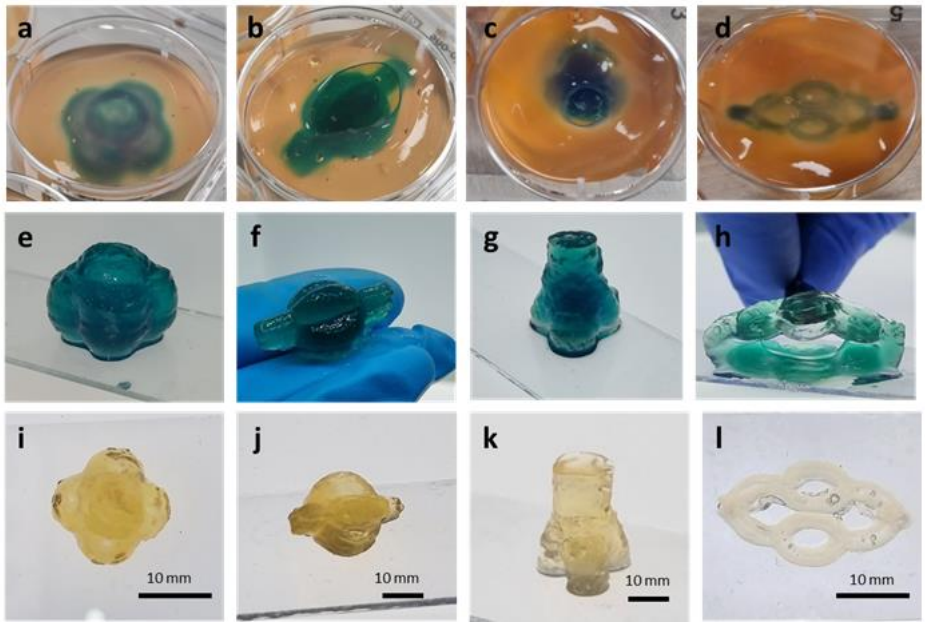

Fig 4 Pictures of complex shape printed and then extracted from a printing bath made of Carbopol dissolved in DMEM

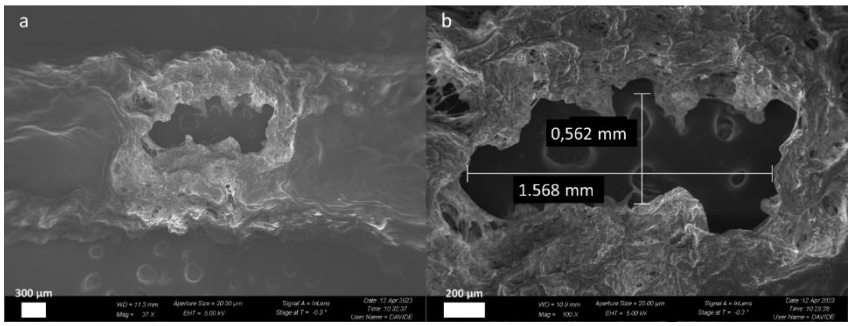

Fig 5 SEM analysis of GelMA construct presenting vessel-like geometry.

3.5. Cell viability and channel seeding

The potentialities of the system were further confirmed by analyzing cell viability after printing. GelMA was loaded with HFF-1 cells at the density of $1x10^6$ cells/ml, after printing the constructs were washed with cell culture medium and cultured for two weeks. As shown in Fig 6, Live&Dead staining was performed after one day of culture to assess printing-related cell death. Interestingly, the viability remained higher than 90% at both time points, indicating the cytocompatibility of the printing process and of the bioink and the supporting bath.

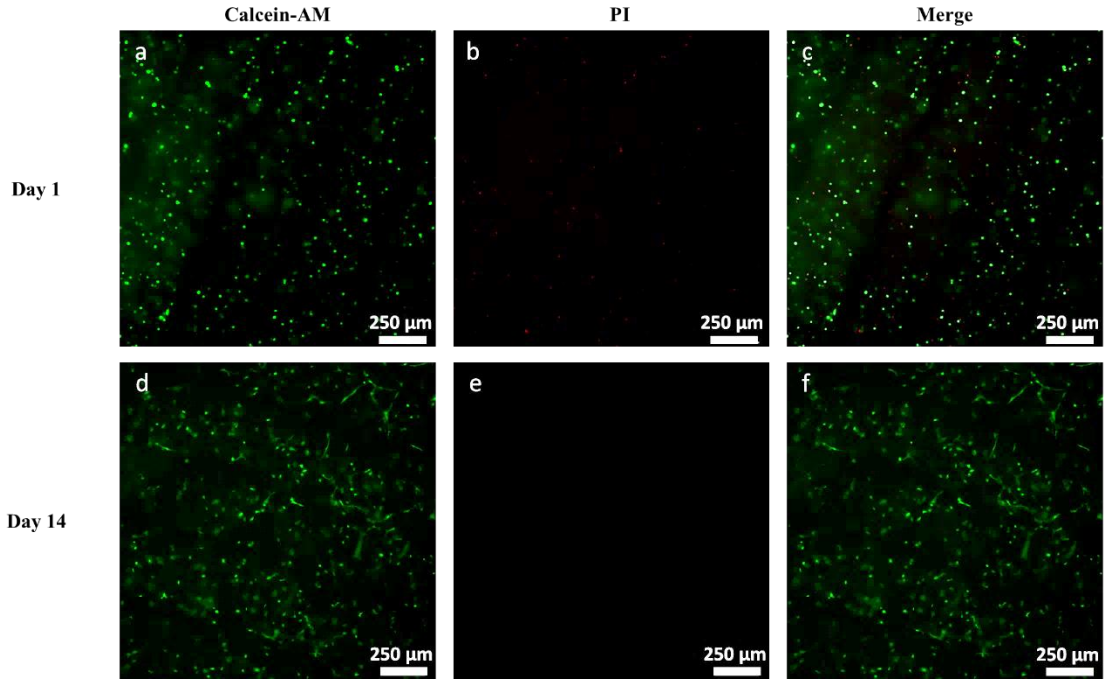

Fig 6 Calcein-AM (green) and PI (red) staining of HFF-1 cells cultured in printed GelMA after 1 day of culture (a,b,c) and after 14 days (d,e,f). The scale bar is set at 250 µm.

Next, samples with an empty channel in the middle were fabricated, mimicking a vessel like geometry. After the 3D bioprinting process and the washing step with DMEM to remove all ETD 2020 NF residues, the resulting channel was filled with 10 µL of $1x10^5$ A549-GFP$^+$ cells. After 48h, the channel was visualized by adding a solution stained by Methylene Blue and as shown in Fig 7 a-c, it was still present and detectable. Moreover, the seeding of fluorescent cells on the wall of the cavity was confirmed by confocal microscopy (Fig 7 d-f). These preliminary experiments demonstrated the feasibility of combining the resolution given by the supporting bath to the need of creating physiological-related culture conditions.

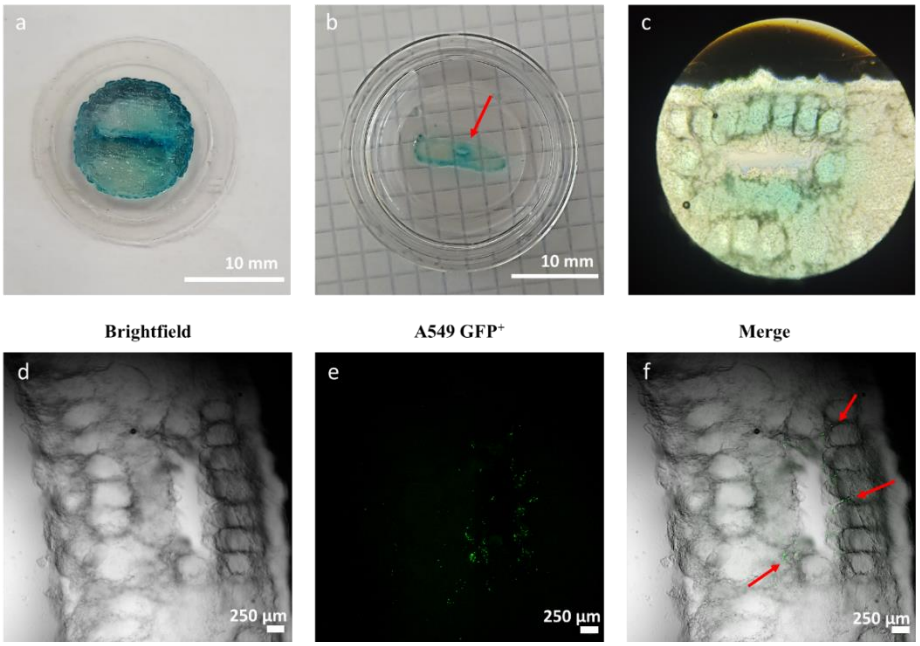

Fig 7 Pictures of scaffold vascularization (a) or view as section (b,c). Confocal microscopy images of A549 GFP$^+$ cells (green) seeded into the channel (d-f)

3. Conclusions

In literature, Carbopol-based formulations prepared in cell culture media, rather than in ddH_2O, has been poorly studied and never been used as supporting bath for the 3D printing of cell-loaded hydrogels. In this work it has been investigated its potential for the printing of GelMA-based bioinks to obtain self-standing scaffold with good resolution also by using more cell-friendly nozzles.

Rheological characterization of GelMA 10% w/v showed how its recovery time was not short enough to have an optimal shape fidelity, as, once extruded, it takes 20 s to recover the 80% of its original value. For this reason, a supporting bath could improve printing outcome by sustaining the ink during the process before the photopolymerization.

ETD 2020 NF formulations, both dissolved in ddH_2O, as control, and cell culture medium, were analyzed in terms of rheological properties and they filled the requirements to be an eligible supporting bath: its storage modulus, G_{bath}', was higher than the one of the bioink, G_{ink}', but not excessive, avoiding the possibility to form cavities with the nozzle passage. ETD 2020 NF also exhibited shear thinning behavior, crucial for a supporting bath material that should behave as a solid when no stress is applied to sustain printed filament, but as liquid where the bioink is being extruded. Further, recovery time was very short; but interestingly, it was a bit longer in ETD 2020 NF in ddH_2O, possibly leading to lower support for the printed structures.

The higher cytocompatibility of ETD 2020 NF in DMEM compared to ETD 2020 NF in ddH_2O, usually employed in literature [23,30,32], together with the lower recovery time and the easier extraction of the scaffold,that leaded to the removal of all the residual Carbopol, made the formulation in cell culture medium the most suitable ones to proceed with further analysis.

Printing of bigger structure and complex shape confirmed that ETD 2020 NF in DMEM was able to sustain self-standing scaffold made of not-photopolymerized GelMA 10% w/v, an outcome that could not be reached with traditional 3D extrusion bioprinting. Further, these results were obtained by employing conical nozzle with larger diameter, which are usually avoided because of their low printing resolution despite the higher cell compatibility.

Since one of the main applications of supporting baths is the production of scaffolds that present channels to mimic a vascular net, the next step was to use the ETD 2020 NF in DMEM support bath to 3D bioprinted vascularized scaffolds. The results showed that not only it was possible to create a through-hole channel, but it was also possible to seed cells inside it. These results, together with the high viability of fibroblasts embedded in the printed constructs, demonstrate that ETD 2020 NF in DMEM bath could be a promising approach to obtain 3D cellularized scaffold with complex shapes, also employing cell-friendly nozzles with larger diameters and bioinks with poor mechanical properties.

References

[1] M. Sun, A. Liu, X. Yang, J. Gong, M. Yu, X. Yao, H. Wang, Y. He, 3D Cell Culture—Can It Be As Popular as 2D Cell Culture?, Adv Nanobiomed Res 1 (2021) 2000066. https://doi.org/10.1002/anbr.202000066.

[2] S. V. Murphy, A. Atala, 3D bioprinting of tissues and organs, Nat Biotechnol 32 (2014) 773–785. https://doi.org/10.1038/nbt.2958.

[3] M. Sun, X. Sun, Z. Wang, S. Guo, G. Yu, H. Yang, Synthesis and properties of gelatin methacryloyl (GelMA) hydrogels and their recent applications in load-bearing tissue, Polymers (Basel) 10 (2018). https://doi.org/10.3390/POLYM10111290.

[4] Y.S. Zhang, R. Oklu, M.R. Dokmeci, A. Khademhosseini, Three-dimensional bioprinting strategies for tissue engineering, Cold Spring Harb Perspect Med 8 (2018). https://doi.org/10.1101/cshperspect.a025718.

[5] S. Ramesh, O.L.A. Harrysson, P.K. Rao, A. Tamayol, D.R. Cormier, Y. Zhang, I. V. Rivero, Extrusion bioprinting: Recent progress, challenges, and future opportunities, Bioprinting 21 (2021). https://doi.org/10.1016/j.bprint.2020.e00116.

[6] J. Groll, J.A. Burdick, D.W. Cho, B. Derby, M. Gelinsky, S.C. Heilshorn, T. Jüngst, J. Malda, V.A. Mironov, K. Nakayama, A. Ovsianikov, W. Sun, S. Takeuchi, J.J. Yoo, T.B.F. Woodfield, A definition

of bioinks and their distinction from biomaterial inks, Biofabrication 11 (2019). https://doi.org/10.1088/1758-5090/aaec52.

[7] S.M. Hull, L.G. Brunel, S.C. Heilshorn, 3D Bioprinting of Cell-Laden Hydrogels for Improved Biological Functionality, Advanced Materials 34 (2022). https://doi.org/10.1002/adma.202103691.

[8] D. Chimene, K.K. Lennox, R.R. Kaunas, A.K. Gaharwar, Advanced Bioinks for 3D Printing: A Materials Science Perspective, Ann Biomed Eng 44 (2016) 2090–2102. https://doi.org/10.1007/s10439-016-1638-y.

[9] I. Pepelanova, K. Kruppa, T. Scheper, A. Lavrentieva, Gelatin-methacryloyl (GelMA) hydrogels with defined degree of functionalization as a versatile toolkit for 3D cell culture and extrusion bioprinting, Bioengineering 5 (2018). https://doi.org/10.3390/bioengineering5030055.

[10] K. Yue, G. Trujillo-de Santiago, M.M. Alvarez, A. Tamayol, N. Annabi, A. Khademhosseini, Synthesis, properties, and biomedical applications of gelatin methacryloyl (GelMA) hydrogels, Biomaterials 73 (2015) 254–271. https://doi.org/10.1016/j.biomaterials.2015.08.045.

[11] X. Ma, C. Yu, P. Wang, W. Xu, X. Wan, C.S.E. Lai, J. Liu, A. Koroleva-Maharajh, S. Chen, Rapid 3D bioprinting of decellularized extracellular matrix with regionally varied mechanical properties and biomimetic microarchitecture, Biomaterials 185 (2018) 310–321. https://doi.org/10.1016/j.biomaterials.2018.09.026.

[12] E. Kaemmerer, F.P.W. Melchels, B.M. Holzapfel, T. Meckel, D.W. Hutmacher, D. Loessner, Gelatine methacrylamide-based hydrogels: An alternative three-dimensional cancer cell culture system, Acta Biomater 10 (2014) 2551–2562. https://doi.org/10.1016/j.actbio.2014.02.035.

[13] A.I. Van Den Bulcke, B. Bogdanov, N. De Rooze, E.H. Schacht, M. Cornelissen, H. Berghmans, Structural and rheological properties of methacrylamide modified gelatin hydrogels, Biomacromolecules 1 (2000) 31–38. https://doi.org/10.1021/bm990017d.

[14] M. Petretta, S. Villata, M.P. Scozzaro, L. Roseti, M. Favero, L. Napione, F. Frascella, C.F. Pirri, B. Grigolo, E. Olivotto, In Vitro Synovial Membrane 3D Model Developed by Volumetric Extrusion Bioprinting, Applied Sciences 13 (2023) 1889. https://doi.org/10.3390/app13031889.

[15] S. Santoni, S.G. Gugliandolo, M. Sponchioni, D. Moscatelli, B.M. Colosimo, 3D bioprinting: current status and trends—a guide to the literature and industrial practice, Biodes Manuf 5 (2022) 14–42. https://doi.org/10.1007/s42242-021-00165-0.

[16] R. Chand, B.S. Muhire, S. Vijayavenkataraman, Computational Fluid Dynamics Assessment of the Effect of Bioprinting Parameters in Extrusion Bioprinting, Int J Bioprint 8 (2022) 45–60. https://doi.org/10.18063/ijb.v8i2.545.

[17] L.G. Brunel, S.M. Hull, S.C. Heilshorn, Engineered assistive materials for 3D bioprinting: support baths and sacrificial inks, Biofabrication 14 (2022). https://doi.org/10.1088/1758-5090/ac6bbe.

[18] B.S. Kim, G. Gao, J.Y. Kim, D.W. Cho, 3D Cell Printing of Perfusable Vascularized Human Skin Equivalent Composed of Epidermis, Dermis, and Hypodermis for Better Structural Recapitulation of Native Skin, Adv Healthc Mater 8 (2019). https://doi.org/10.1002/adhm.201801019.

[19] N.Y.C. Lin, K.A. Homan, S.S. Robinson, D.B. Kolesky, N. Duarte, A. Moisan, J.A. Lewis, Renal reabsorption in 3D vascularized proximal tubule models, Proc Natl Acad Sci U S A 116 (2019) 5399–5404. https://doi.org/10.1073/pnas.1815208116.

[20] L. Ning, R. Mehta, C. Cao, A. Theus, M. Tomov, N. Zhu, E.R. Weeks, H. Bauser-Heaton, V. Serpooshan, Embedded 3D Bioprinting of Gelatin Methacryloyl-Based Constructs with Highly Tunable Structural Fidelity, ACS Appl Mater Interfaces 12 (2020) 44563–44577. https://doi.org/10.1021/acsami.0c15078.

[21] Y. Li, Q. Mao, K. Xu, H. Yang, Y. Huang, J. Yin, Vat photopolymerization bioprinting with a dynamic support bath, Addit Manuf 69 (2023) 103533. https://doi.org/10.1016/j.addma.2023.103533.

[22] Q. Li, Z. Jiang, L. Ma, J. Yin, Z. Gao, L. Shen, H. Yang, Z. Cui, H. Ye, H. Zhou, A versatile embedding medium for freeform bioprinting with multi-crosslinking methods, Biofabrication 14 (2022). https://doi.org/10.1088/1758-5090/ac7909.

[23] T. Bhattacharjee, S.M. Zehnder, K.G. Rowe, S. Jain, R.M. Nixon, W.G. Sawyer, T.E. Angelini, Writing in the granular gel medium, Sci Adv 1 (2015). https://doi.org/10.1126/sciadv.1500655.

[24] J.T. Muth, D.M. Vogt, R.L. Truby, Y. Mengüç, D.B. Kolesky, R.J. Wood, J.A. Lewis, Embedded 3D printing of strain sensors within highly stretchable elastomers, Advanced Materials 26 (2014) 6307–6312. https://doi.org/10.1002/adma.201400334.

[25] A.K. Grosskopf, R.L. Truby, H. Kim, A. Perazzo, J.A. Lewis, H.A. Stone, Viscoplastic Matrix Materials for Embedded 3D Printing, ACS Appl Mater Interfaces 10 (2018) 23353–23361. https://doi.org/10.1021/acsami.7b19818.

[26] Q. Wu, K. Song, D. Zhang, B. Ren, M. Sole-Gras, Y. Huang, J. Yin, Embedded extrusion printing in yield-stress-fluid baths, Matter 5 (2022) 3775–3806. https://doi.org/10.1016/J.MATT.2022.09.003.

[27] A.Z. Nelson, K.S. Schweizer, B.M. Rauzan, R.G. Nuzzo, J. Vermant, R.H. Ewoldt, Designing and transforming yield-stress fluids, Curr Opin Solid State Mater Sci 23 (2019). https://doi.org/10.1016/j.cossms.2019.06.002.

[28] D. Baruffaldi, C.F. Pirri, F. Frascella, 3D bioprinting of cell-laden carbopol bioinks, Bioprinting 22 (2021). https://doi.org/10.1016/j.bprint.2021.e00135.

[29] T. Bhattacharjee, S.M. Zehnder, K.G. Rowe, S. Jain, R.M. Nixon, W.G. Sawyer, T.E. Angelini, Writing in the granular gel medium, Sci Adv 1 (2015). https://doi.org/10.1126/sciadv.1500655.

[30] J. Dairaghi, D. Rogozea, R. Cadle, J. Bustamante, L. Moldovan, H.I. Petrache, N.I. Moldovan, 3D Printing of Human Ossicle Models for the Biofabrication of Personalized Middle Ear Prostheses, Applied Sciences (Switzerland) 12 (2022). https://doi.org/10.3390/app122111015.

[31] Y. Jin, A. Compaan, T. Bhattacharjee, Y. Huang, Granular gel support-enabled extrusion of three-dimensional alginate and cellular structures, Biofabrication 8 (2016). https://doi.org/10.1088/1758-5090/8/2/025016.

[32] C.S. O'Bryan, T. Bhattacharjee, S.L. Marshall, W. Gregory Sawyer, T.E. Angelini, Commercially available microgels for 3D bioprinting, Bioprinting 11 (2018). https://doi.org/10.1016/j.bprint.2018.e00037.

[33] S.N. Ho, Intracellular water homeostasis and the mammalian cellular osmotic stress response, J Cell Physiol 206 (2006) 9–15. https://doi.org/10.1002/jcp.20445.

[34] T. Bhattacharjee, C.J. Gil, S.L. Marshall, J.M. Urueña, C.S. O'Bryan, M. Carstens, B. Keselowsky, G.D. Palmer, S. Ghivizzani, C.P. Gibbs, W.G. Sawyer, T.E. Angelini, Liquid-like Solids Support Cells in 3D, ACS Biomater Sci Eng 2 (2016) 1787–1795. https://doi.org/10.1021/acsbiomaterials.6b00218.

[35] S. Villata, M. Canta, D. Baruffaldi, I. Roppolo, C.F. Pirri, F. Frascella, 3D bioprinted GelMA platform for the production of lung tumor spheroids, Bioprinting 36 (2023). https://doi.org/10.1016/j.bprint.2023.e00310.

[36] L. Ning, C.J. Gil, B. Hwang, A.S. Theus, L. Perez, M.L. Tomov, H. Bauser-Heaton, V. Serpooshan, Biomechanical factors in three-dimensional tissue bioprinting, Appl Phys Rev 7 (2020). https://doi.org/10.1063/5.0023206.

[37] N. Paxton, W. Smolan, T. Böck, F. Melchels, J. Groll, T. Jungst, Proposal to assess printability of bioinks for extrusion-based bioprinting and evaluation of rheological properties governing bioprintability, Biofabrication 9 (2017). https://doi.org/10.1088/1758-5090/aa8dd8.

[38] L.G. Brunel, S.M. Hull, S.C. Heilshorn, Engineered assistive materials for 3D bioprinting: support baths and sacrificial inks, Biofabrication 14 (2022). https://doi.org/https://doi.org/10.1088/1758-5090/ac6bbe.

[39] D. Nothdurfter, C. Ploner, D.C. Coraça-Huber, D. Wilflingseder, T. Müller, M. Hermann, J. Hagenbuchner, M.J. Ausserlechner, 3D bioprinted, vascularized neuroblastoma tumor environment in fluidic chip devices for precision medicine drug testing, Biofabrication 14 (2022). https://doi.org/10.1088/1758-5090/ac5fb7.